Applied Mathematics & Information Sciences
An International Journal

http://dx.doi.org/10.18576/amis/140113

Certain Mathematical Investigations on Prenatal Down Syndrome Detection using ANFIS Classification Approach

S. Saranya[1,*] *and S. Sudha*[2]

[1]Faculty of Electronics and Communication Engineering, Saveetha School of Engineering, Chennai, India
[2]Faculty of Electronics and Communication Engineering, Easwari Engineering College, Chennai, India

Received: 10 Oct. 2018, Revised: 16 Dec. 2018, Accepted: 8 Jun. 2019
Published online: 1 Jan. 2020

Abstract: The genetic disorder of foetus leads to the formation of Down Syndrome (DS) which can be screened manually by screening the first and second trimester ultra sonogram images. This can be fully automated with the help of computer-aided approaches proposed in this paper. The DS can be screened by enhancing the foetus image using Adaptive histogram equalization technique. Then, Gabor multi resolution transform is applied on the enhanced foetus image in order to convert the spatial domain foetus image into multi resolution foetus image. The features as Effective Binary Pattern (EBP), Grey Level Occurrence Matrix (GLCM) and Local Derivative Pattern (LDP) are extracted from the enhanced Gabor transformed foetus image and then these features are trained and classified using Adaptive Neural Fuzzy Inference System (ANFIS) classifier, which classifies the foetus image into either normal or abnormal. Further, morphological-based segmentation technique is applied on the abnormal classified foetus image to segment the nasal bone region. The segmented nasal bone region is compared with clinical diagnosis results to detect DS in foetus image. The performance of the proposed DS detection system is analyzed in terms of sensitivity, specificity, positive predictive value, negative predictive value and accuracy

Keywords: Down Syndrome, Features, Enhancement, Foetus Images, Classifier

1 Introduction

Down syndrome (otherwise called as trisomy 21) is the disorder of the foetus which can be identified by examining the ultra sonogram images at first and second trimester stages. This can be occurred at the ratio of 1:800 live births in world. The integration of extra chromosome in 23 human chromosome leads to genetic disorder in foetus, which is the main cause of DS. The maternal duration and the morphological analysis of nuchal translucency in foetus are determined by first and second trimester stages Deivasigamani et al. [1]. The DS can be screened by analyzing the trimester stage images manually which achieves 85% of average detection rate with 5% to 10% error rate with respect to different radiologist.

The nasal bone (small bifid structure in foetus) forms in the foetus after first trimester stage of the foetus. The first trimester images can be obtained between 11 and 14 weeks of the foetus development. There is no nasal bone formed in first trimester stage. The second trimester images can be obtained between 15 and 20 weeks of the foetus development with the growth of nasal bone. The radiologist determines the length of the nasal bone at second trimester stage for DS detection at an earlier stage. Detection of DS through the nasal bone analysis produces 97% of detection rate with 5% error rate as stated in Cicero et al. [2]. Cicero et al. [2] analyzed the impact of nasal bone length on the DS detection process in first trimester stage. The author found that there is no significance difference between the normal foetus and DS affected foetus.

Due to this limitation, the researchers concentrated their research on impact of nasal bone length in second trimester stages for an efficient detection of DS. The length of the nasal bone in foetus at second trimester determines DS at an earlier stage as defined in Nicolaides et al. [3]. The nasal bone length varies with respect to different population as indicated in many studies by Cicero et al. [2]; Nicolaides et al. [3]; Rajanna et al. [4];

* Corresponding author e-mail: nimmycharan@gmail.com

Rafeek and Gunasundari [5]. Hence, the determination of reference nasal bone length cannot be fixed due to its variance with respect to different population.

The nasal region in foetus face consists of nasal bone and nasal tip which can be separated by nasal skin as shown in Figure 1. The nasal bone has thick tissues where as the nasal tip has thin tissues. The length of nasal bone should be between 1.1 mm to 1.9 mm at 11th week of foetus stage and it varies between 1.1 mm to 2.5 mm at 12th week of foetus and it also varies between 1.5 mm and 2.6 mm at 13th week of the foetus Chitkasaem et al. [6]. The average nuchal translucency thickness is around 1.2 mm as reported in Chitkasaem et al. [6].

Fig. 1: Illustration of nasal bone in ultra sonogram image

Section 2 discusses various conventional methodologies for the detection of DS in foetus images and Section 3 proposes an efficient methodology for DS detection. Section 4 discusses the experimental results of the proposed method with conventional methods. Section 5 concludes the paper.

2 Literature Survey

Rajanna et al. [4] studied on Pinna length measurement and its association with chromosomal disorders has been made. The authors analyzed the linear relationship between the pinna length and the gestational age. Rafeek and Gunasundari [5] used hybrid despeckling filter to detect and remove the noises in the ultra sound foetus image. The authors applied Sobel edge detection method on denoised foetus image to detect the edge variations in foetus and then watershed segmentation technique was applied to identify the region of interest for the abnormal nasal bone in second trimester images. The authors also used neural network classifier to detect and classify the nasal bone in foetus images. Anjit and Rishidas [7] applied Discrete Cosine Transform (DCT) transform on ultra sonogram trimester images in order to extract the texture features. The authors trained and classified these features using feed forward back propagation neural networks. Senat et al. [8] used interoperator variability measurement procedure to screen the length of the nasal bone in various foetus images to analyze its abnormalities. The authors applied their diagnosis procedure on foetus images ate 11 to 14 weeks period. Sonek et al. [9] developed Down syndrome detection procedure from ultra sonogram foetus images. The authors applied various enhancement techniques to enhance the internal view of the foetus at different stages of foetus age. The authors achieved 67% of sensitivity and 72% of specificity with respect to ground truth sonogram images. Cicero et al. [2] analyzed the DS detection process by determining the length of the nasal bone in foetus from the week between 11 and 14. The authors developed many screening techniques for the earlier detection of DS in foetus at different trimester stages of the foetus with respect to different population.

3 Proposed Methodology

In this article, ANFIS classification approach-based foetus screening for DS detection is proposed. The proposed method is applied to both foetus images with first trimester and second trimester period. The foetus image is enhanced in preprocessing stage in order to highlight the internal parts of the foetus and then Gabor transform is applied to produce the multi resolution image. Further, features are extracted from Gabor-transformed image and these extracted features are classified using ANFIS classifier in order to classify the foetus image into either normal or DS-affected foetus image. The proposed flow of this article is illustrated in Figure 2.

3.1 Preprocessing

In this paper, the foetus image is resized into 256×256 as image width and height. Contrast-Limited Adaptive Histogram Equalization (CLAHE) technique (Neethu et al. 2013) is used for enhancement of foetus image for better classification. This technique enhances the contrast of the grey scale values of the pixels in resized foetus image.

Step 1: The foetus image is split into 3×3 contextual regions.

Step 2: Find the minimum intensity pixel ($I_{\min}$) in 3×3 contextual region.

$$I_{\min} = \text{Minimum(pixels in } 3 \times 3 \text{ regions)} \quad (1)$$

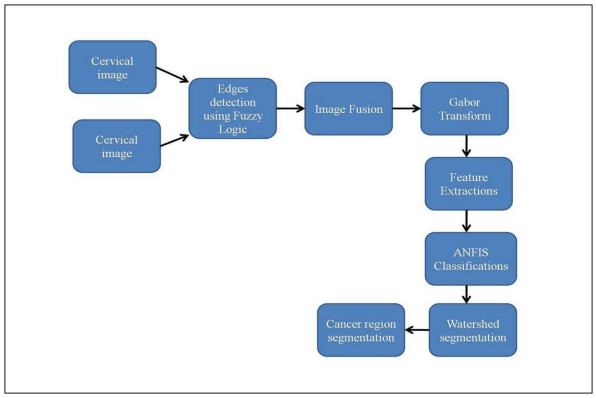

Fig. 2: Proposed down syndrome detection process

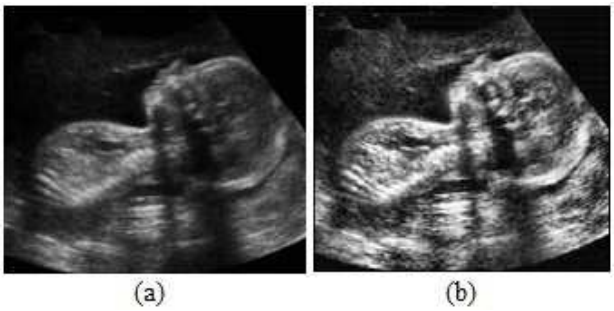

Fig. 3: (a) Source foetus image (b) Preprocessed foetus image

Step 3: Find the maximum intensity pixel ($I_{\max}$) in 3×3 contextual region.

$$I_{\max} = \text{Maximum(pixels in } 3 \times 3 \text{ regions)} \quad (2)$$

Step 4: Determine the probability density function (I_{PDF}) of the corresponding contextual region.

Step 5: Find the enhanced pixel intensity using the following equation,

$$I_{\text{Enhance}} = (I_{\max} - I_{\min}) \times I_{\text{PDF}} \quad (3)$$

Step 6: Repeat steps 2 to 5 for next 3×3 contextual regions till the end of pixel in foetus image.

Figure 3 shows the preprocessed foetus image in first trimester period.

3.2 Gabor Transform

Transformation is applied on the spatial domain image which can be converted into frequency domain image. In this article, multi-resolution transform is applied on the foetus image which converts the spatial domain foetus image into multi resolution domain image with respect to different scale and orientations. The Gabor kernel can be represented as Equation 5 the convolution of complex sinusoidal carrier and 2D Gaussian shaped kernel function.

$$G(x,y) = S(x,y) \times g(x,y) \quad (4)$$

where, $S(x,y)$ is the pre-processed foetus image and $g(x,y)$ is the Gabor kernel. The 2D Gabor kernel can be given as,

$$G(x,y) = \frac{k}{ab}\exp\left(-j2\pi(x_0(\mu-\mu_0)+y_0(\nu-\nu_o))+P\right) \times \exp\left(-\pi\frac{(\mu-\mu_0)^2}{a^2}+\frac{(\nu-\nu_0)^2}{b^2}\right) \quad (5)$$

where, the scale of the Gabor kernel is represented as k and it varies from 1 to 5, the scales of the Gaussian envelope is depicted as a and b. The coordinates of the Gaussian envelope are x_0 and y_0. The polar form of coordinates for the Gaussian envelope is noted as μ_0 and ν_0. P is the phase of the sinusoidal carrier of the Gabor kernel. The average Gaussian envelope is depicted as μ. The magnitude of the Gabor kernel is,

$$|G(x,y)| = \frac{k}{ab}\exp\left(-\pi\frac{(\mu-\mu_0)^2}{a^2}+\frac{(\nu-\nu_0)^2}{b^2}\right) \quad (6)$$

The phase of the Gabor kernel is,

$$G(x,y) = -2\pi(x_0(\mu-\mu_0)+y_0(\nu-\nu_o))+P \quad (7)$$

This Gabor kernel is convolved with pre-processed foetus image as depicted in equation,

$$GI = I(x,y) \times G(x,y) \quad (8)$$

The magnitude of the Gabor transformed foetus image is given as,

$$|GI| = \sqrt{(\text{Real}(GI)^2 + \text{Imaginary}(GI)^2)} \quad (9)$$

The magnitude of the Gabor transformed foetus image and its orientation image is depicted in Figure 4.

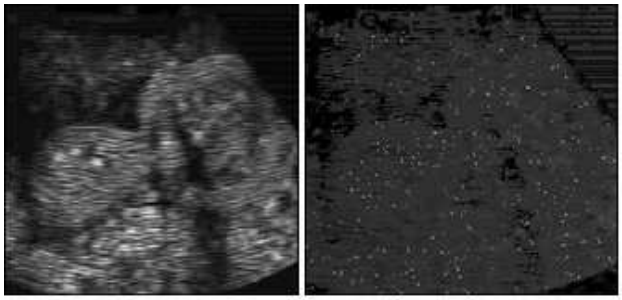

(a) (b)

Fig. 4: (a) Magnitude of Gabor transformed image (b) Orientation image

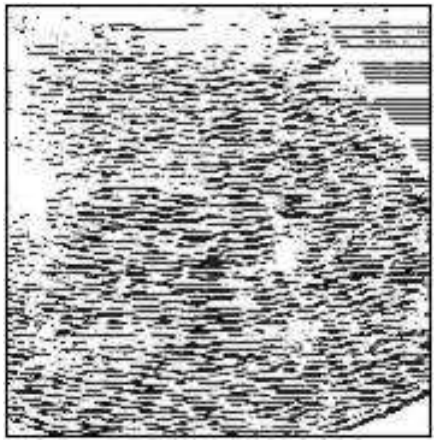

Fig. 5: LBP feature image

3.3 Feature Extraction

The DS affected foetus image is differentiated from normal foetus image through feature extraction process. In this article, GLCM, Effective Binary Pattern (EBP) and LDP features are extracted from the Gabor transformed foetus image.

3.4 EBP features

In this paper, EBP feature is extracted from the pre-processed foetus image, which is the modification of LBP features. In case of LBP feature extraction procedure, the middle pixel value in 3×3 sub window is compared with surrounding eight pixel values. The subtraction between middle pixel and the surrounding pixel value is tested for forming LBP feature. The LBP value becomes one if the subtraction value is positive and the LBP value becomes zero if the subtraction value is negative. In this way, these eight binary values are converted into decimal value which lies between 0 and 255. In case of EBP, the decimal value is considered for feature if and only it contains minimum of two transitions in eight binary patterns. Otherwise, the feature is considered as zero. Hence, the feature content in EBP image is reduced as depicted in Figure 5.

The equation for *EBP* feature extraction process is given as,

$$EBP = \sum_{p=1}^{P} 2^p Y(C - S_v) \tag{10}$$

whereas, C is the centre pixel in 3×3 sub window and S_p is the surrounding pixels in 3×3 sub window with P number of surrounding pixels.

3.5 LDP

The extension of LBP is otherwise called as LDP which can be computed based on its different orientation. In this paper, second-order derivative at the orientations of 0°, 45°, 90°, and 135° is used in order to compute LDP feature set. The LDP pattern has four features for the above four different orientation.

The LDP feature for a specific orientation is computed in nth order which is given as,

$$LDR_{\phi}^{(n-1)}(r_c)|_{(\phi=0°,45°,90°,135°)} \tag{11}$$

where, k represents the order of the feature and it is set to 2 in this paper. r_c is the center pixel in 3×3 sub window. The nth order LDP feature is computed using the following equation.

$$LDR_{\phi}^{k}(r_c) = \sum_{p=1}^{P} 2^{(p-1)} x f_1(I_{\phi}^{(k-1)}(r_c), I_{\phi}^{(k-1)}(r_p))|_{p=8} \tag{12}$$

where, $f_1(x,y) = \begin{cases} 1, & \text{for } r_p \text{ and } r_c \geq 0 \\ 0, & \text{otherwise} \end{cases}$

P represents the number of surrounding pixels and p varies from 1 to 8. The extracted LDP feature is shown in Figure 6. Figure 6(a) shows the LDP feature extracted image at 0° orientation, Figure 6(b) shows the LDP feature extracted image at 45° orientation, Figure 6(c) shows the LDP feature extracted image at 90° orientation and Figure 6(d) shows the LDP feature extracted image at 135° orientation.

3.6 GLCM Features

In this paper, GLCM features as contrast, energy, entropy and correlation are extracted from the Gabor-transformed image.

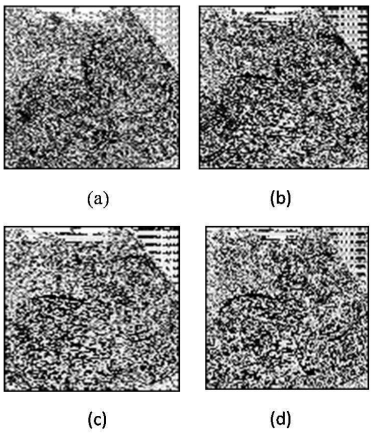

Fig. 6: LDP feature images at (a) 0° orientation (b) 45° orientation (c) 90° orientation (d) 135° orientation

Energy feature $\quad \text{Energy} = \sum_{i,j=0}^{N-1} P_{ij}^2$

Entropy feature $\quad \text{Entropy} = \sum_{i,j=0}^{N-1} -\ln(P_{ij})P_{ij}$

Contrast feature $\quad \text{Contrast} = \sum_{i,j=0}^{N-1} P_{ij}(i-j)^2$

Correlation feature $\quad \text{Correlation} = \sum_{i,j=0}^{N-1} P_{ij}\frac{(i-\mu)(j-\mu)}{\sigma^2}$

where

$P_{ij} =$ Element i, j of the normalized symmetrical GLCM.

$N =$ Number of gray levels in the image as specified by **Number of levels** in under **Quantizated** on the GLCM.

$\mu =$ the GLCM mean (being an estimate of the intensity of all pixels in the relationships that contributed to the GLCM), calculated as: $\mu = \sum_{i,j=0}^{N-1} iP_{ij}$.

The GLCM matrix is constructed at the orientation of pixels with 45°.

3.7 Classification and segmentation

Classification of DS affected foetus or normal foetus is important for improving the detection accuracy of the DS detection system. SVM and Neural Networks are the conventional methods for the automatic detection and classification of DS affected foetus from normal foetus images. The main limitation of these conventional methods is its low detection and classification rate. Hence, ANFIS classification approach is used in this article for the automatic detection and classification of foetus images into either DS affected foetus or not. Initially, the features are extracted from normal foetus and DS affected foetus and given to the training mode of this classifier which produces trained pattern. Further, the features are extracted from the test foetus image and it is classified with respect to the trained patterns in classification mode of this classifier. The classification result is either zero or one. The zero classification result leads to the detection of normal foetus image and classification result 'one' leads to the detection of DS affected foetus image. Figure 7(a) shows the normal foetus images and Figure 7(b) shows the DS affected foetus images.

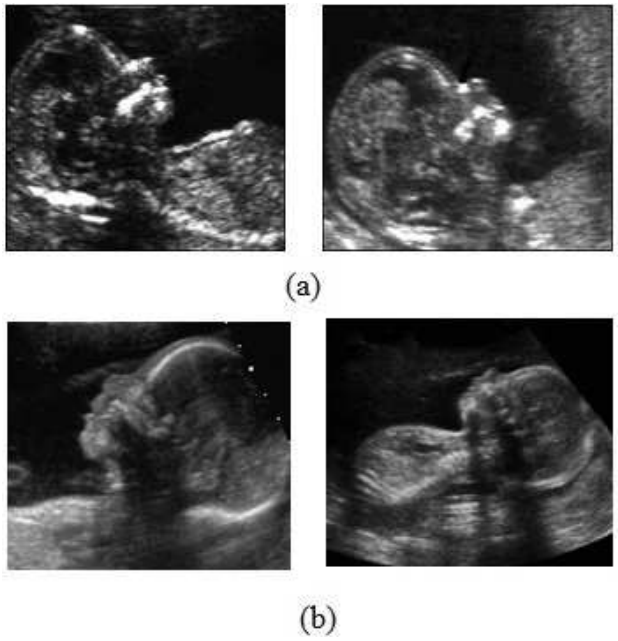

Fig. 7: (a) Normal foetus images (b) DS affected foetus images

The nasal bone is segmented from the DS affected foetus image for diagnosing the DS with respect to first and second trimester stages.Morphological opening and closing is applied on the classified foetus image. The morphological closed image is subtracted from morphological opened image in order to segment the nasal bone in classified foetus image. The Region Of Interest (ROI) of the nasal bone in classified image is shown in Figure 8(a) and it is marked in Figure 8(b).

The morphological parameters as Area, Perimeter, Width and Height are determined from the segmented nasal bone region.Table 1 shows the morphological

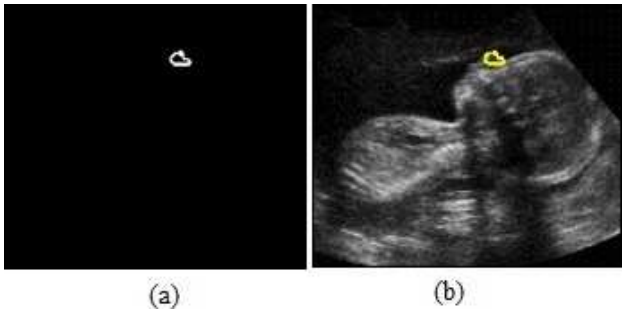

Fig. 8: (a) ROI extracted image (b) Nasal bone region segmented image

analysis of segmented nasal bone in classified foetus image. The clinical and experimental values of the segmented nasal bone are shown in Table 1.

Table 1: Morphological analysis of segmented nasal bone in classified foetus image

	Segmented nasal bone	
Morphological parameters	Clinical values (Cicero et al. 2001)	Experimental results
Area (mm^2)	[310, 410]	393
Perimeter (mm)	[81, 90]	84.97
Width (mm)	[29, 31]	30.74
Height (mm)	[17, 18]	17.37

Table 2: GLCM features for normal and abnormal foetus images

	GLCM feature values	
GLCM features	Normal image	Abnormal image
Energy	2.24×10^{-5}	2.13×10^{-5}
Entropy	1.08×10^{1}	1.38×10^{1}
Homogeneity	3.46×10^{-2}	3.95×10^{-2}
Contrast	9.62×10^{3}	9.97×10^{3}
Correlation	-5.3×10^{-2}	1.14×10^{-1}

4 Results and Discussion

In this article, MATLAB software is used to simulate the proposed DS detection system and it takes 5 seconds per foetus image classification. The proposed system is analyzed with the parameter detection rate which is defined as the ratio between the numbers of correctly-detected DS affected foetus images and the total number of foetus images used. In this article, the 20 DS affected foetus sonographic image(no nasal bone) which is obtained in first trimester (11–14 weeks) is tested with the proposed Down syndrome detection stated in [10].

The proposed method incorporating EBP and LDP features detects 17 foetus sonograhic images with no nasal bone and achieves 85% detection rate for the first trimester images. The proposed method incorporating GLCM with EBP and LDP features detects 19 foetus sonograhic images with no nasal bone and achieves 95% detection rate for the first trimester images. Hence, the impact of GLCM features is important for improving the detection rate. Further, the proposed method is also applied to 30 DS affected foetus images (which has irregular nasal bone length) in second trimester (12–20 weeks) and achieves 96.6% of detection rate by identifying 29 DS-affected foetus images. Hence, the average detection rate of the proposed system is 95.8%. Table 3 shows the comparisons of detection for the proposed method with conventional methodologies.

Table 3: Comparisons of detection for the proposed method with conventional methodologies

Methodology	Number of DS affected foetus images	Detection rate (%)
Proposed method	50	95.8
Chitkasaem et al. (2013)	50	91.7
O'Leary et al. (2006)	50	87.6
Cicero et al. (2001)	50	73

The performance of the proposed down syndrome detection methodology is analyzed with respect to its ground truth images in terms of sensitivity, specificity, Positive Predictive Value, Negative Predictive Value and accuracy. The ground truth images used in this article are obtained from expert radiologist and physician. The performance evaluation parameters of the proposed down syndrome detection and diagnosis system are depicted in the following equations.

$$\text{Sensitivity } (Se) = \frac{TP}{(TP+FN)} \tag{13}$$

$$\text{Specificity } (Sp) = \frac{TN}{(TN+FP)} \tag{14}$$

$$\text{Positive Predictive Value } (PPV) = \frac{TP}{(TP+FP)} \tag{15}$$

$$\text{Negative Predictive Value } (NPV) = \frac{TN}{(TN+FN)} \tag{16}$$

$$\text{Accuracy } (Acc) = \frac{(TP+TN)}{(TP+FN+TN+FP)} \tag{17}$$

where, TP is True Positive which indicates the total number of correctly-detected nasal bone pixels, TN is True Negative which indicates the total number of correctly-detected non-nasal bone pixels, FP is False Positive which indicates the number of wrongly-detected

nasal bone pixels and *FN* is False Negative which indicates the number of wrongly detected non-nasal bone pixels. These parameters are computed using ground truth images and they vary between 0 and 255. The performance evaluation of the proposed nasal bone detection system is depicted in Table 4.

Table 4: Performance evaluation of proposed nasal bone detection system

Performance analysis parameters	Experimental results(%)
Sensitivity (Se)	82.66
Specificity (Sp)	99.94
Positive Predictive Value (PPV)	86.98
Negative Predictive Value (NPV)	99.92
Accuracy	99.97

Table 5 shows the performance comparisons of nasal bone segmentation for the proposed method stated in this paper with conventional methods as Chitkasaem et al. [6], O'Leary et al. [11] and Cicero et al. [2]. The proposed methodology achieves 82.66% of sensitivity, 99.94% of specificity and 99.97% of accuracy, while the conventional method Chitkasaem et al. [6] achieved 72.11% of sensitivity, 93.29% of specificity and 91.38% of accuracy. O'Leary et al. [11] achieved 76.45% of sensitivity, 94.34% of specificity and 93.72% of accuracy. Cicero et al. [2] achieved 78.63% of sensitivity, 96.19% of specificity and 95.57% of accuracy.

Table 5: Performance comparisons of nasal bone segmentation

Methodology	Sensitivity (%)	Specificity (%)	Accuracy (%)
Proposed method (this work)	82.66	99.94	99.97
Chitkasaem et al. (2013)	72.11	93.29	91.38
O'Leary et al. (2006)	76.45	94.34	93.72
Cicero et al. (2001)	78.63	96.19	95.57

5 Conclusion

This paper presents the computer-aided approach for the detection of DS in foetus trimester ultra sound images. The proposed system consists of preprocessing, Gabor transform, feature extraction and classifications. The foetus image is enhanced in preprocessing stage and then the spatial domain foetus image is converted into multi-resolution image using Gabor transform. Then, the features are extracted from Gabor transformed foetus image and these features are trained and classified using ANFIS classifier. Further, morphological operations are applied on the classified foetus image in order to segment the nasal bone. The proposed method detects 19 foetus ultra sonogram images with no nasal bone and achieves 95% detection rate for the first trimester images. Further, the proposed method is also applied to 30 DS affected foetus images (which has irregular nasal bone length) in second trimester (12–20 weeks) and achieves 96.6% of detection rate by identifying 29 DS affected foetus images. The proposed methodology achieves 82.66% of sensitivity, 99.94% of specificity and 99.97% of accuracy for the segmentation of nasal bone with respect to ground truth images. In future, this research work can be used to detect the cancer in foetus images using ultra sonogram images.

References

[1] S. Deivasigamani, C. Senthilpari, and Wong Hin Yong, Classification of focal and nonfocal EEG signals using ANFIS classifier for epilepsy detection, *International Journal of Imaging Systems and Technology*, **26**(4), 277–283 (2016).

[2] S. Cicero, P. Curcio, A. Papageorghiou, J. Sonek and K. Nicolaides, *Absence of nasal bone in foetuses with trisomy 21 at 11–14 weeks gestation: an observational study*, Lancet, 1665–1667 (2001).

[3] K.H. Nicolaides, Nuchal translucency and other first-trimester sonographic markers of chromosomal abnormalities, *American Journal of Obstetrics Gynecolgy*, 45-–67 (2004).

[4] Rajanna, Ambresh, Manikantan and Sharath, Antenatal Ultrasound Fetal Pinna Measurement and Evolving Nomogram in South Indian Population in Normal Pregnancies, *International Journal of Anatomy, Radiology and Surgery*, 21–26 (2016).

[5] T. Rafeek and A. Gunasundari, Reliable Non invasive First Trimester Screening Test Using Image processing and Artificial Neural Network, *International Journal of Engineering Research and Applications*, **3**, 662–668 (2013).

[6] S. Chitkasaem, P. Ninlapa, K. Ounjai, S. Thitima, H. Tharangrut and P. Savitree , Reliability of fetal nasal bone length measurement at 11–14 weeks of gestation, *BMC Pregnancy and Childbirth*, 7–13 (2013).

[7] T.A. Anjit and S. Rishidas, *Identification of nasal bone for the early detection of down syndrome using Back Propagation Neural Network*, International Conference on Communications and Signal Processing, Calicut, 136–140 (2011).

[8] M.V. Senat, J.P. Bernard and M. Boulvain, Intra- and inter-operator variability in fetal nasal bone assessment at 11–14 weeks of gestation, *Ultrasound Obstet. Gynecol.*, **22**, 138–141 (2003).

[9] J.D. Sonek, K.H. Nicolaides and D. Helbing, Prenatal ultrasonographic diagnosis of nasal bone abnormalities in three foetuses with Down syndrome, *Am. J. Obstet. Gynecol.*, **186**, 139–141 (2002).

[10] Database, Available at: https://fetalmedicine.org/nuchal-translucency-scan.

[11] P. O'Leary, N. Breheny, J.E. Dickinson, C. Bower, J. Goldblatt, B. Hewitt, A.Murch and R. Stock, First-trimester combined screening for Down syndrome and other fetal anomalies, *Obstet. Gynecol.*, **107**, 869–876 (2006).

[12] H.O. Ilhan Celik, and A. Elbir, *Detection and estimation of down syndrome genes by machine learning techniques*, 25th IEEE Signal Processing and Communications, Applications Conference (SIU), Antalya, 253–262 (2017).
[13] M. Sasi, and V.K. Jayasree, Contrast Limited Adaptive Histogram Equalization for Qualitative Enhancement of Myocardial Perfusion Images, *Scientific Research Engineering*, 326–331 (2013).
[14] V.K. Vincy Devi and R. Rajesh, *A study on Down syndrome detection based on Artificial Neural Network in Ultra sonogram images*, IEEE International Conference on Data Mining and Advanced Computing (SAPIENCE), Ernakulam, 204–209 (2016).

S. Saranya is currently an Assistant Professor of Information Communication Engineering at Saveetha University. She has completed her Masters in Communication Systems at Easwari Engineering College (Anna University). Her main research interests are: Mathematical model in biomedical images, artificial intelligence, neural networks. She has published many papers in international and national journals.

S. Sudha is working as Professor in the Department of Information Communication Engineering at Easwari Engineering College (Anna University) and received PhD degree in Information Communication Engineering. Her research interests are in the areas of imaging, wireless communication, neural networks and embedded systems. She has published more than 100 research articles in reputed international journals in engineering sciences. She is referee and editor of many international journals. Currently she is guiding 8 research scholars.